# Structure and Properties of *p*-Aminophenoxyl Radical

**Daniel M. Chipman**

*Radiation Laboratory, University of Notre Dame, Notre Dame, Indiana 46556*

*Received: August 10, 1999; In Final Form: September 23, 1999*

The geometrical structure, fundamental vibrational frequencies, and isotropic hyperfine coupling constants of *p*-aminophenoxyl radical are investigated by means of electronic structure calculations. Neither Hartree−Fock nor full $\pi$-space multiconfigurational self-consistent-field approaches are able to provide a satisfactory account of the experimentally observed vibrational frequencies. This is due mostly to not allowing the CN bond to participate sufficiently in the conjugation, thereby also allowing pyramidalization at the nitrogen site. Density functional methods, on the other hand, do give a reasonable description of the vibrational frequencies. Consideration of solvation effects by incorporation of four hydrogen-bonded water molecules, two at the oxygen site and two at the amino site, strengthens the CN bond and promotes planarity of the radical. With inclusion of solvent, the density functional vibrational frequencies are further improved to come into very good agreement with experimental results in water. For the most part, hyperfine coupling constants are in satisfactory agreement with experiment. Vibrational averaging over large amplitude pyramidalization and torsional motions of the amino group atoms leads to only modest corrections to the hyperfine couplings and gives no support to an experimental report of significant temperature dependence of the amino hydrogen couplings in a presumably closely related derivative. However, averaging over these motions does give a good rationalization of the observed deuterium isotope shift in the amino hydrogen coupling.

## Introduction

Experimental studies on *p*-aminophenoxyl (PAP) radical have provided considerable information on the magnetic isotropic hyperfine coupling constants[1−4] (hfcc), the p$K_a$ of the radical cation conjugate acid,[5] the redox potential,[6] the vibrational frequencies,[7−10] the optical absorption spectrum,[8] and the OH bond dissociation energy of the parent *p*-aminophenol.[11,12] In addition, theoretical studies have been reported on the hydrogen exchange reactions with peroxides,[13] the geometrical structure,[14,15] the vibrational frequencies and spin distribution,[14] and the *p*-aminophenol OH bond dissociation energy.[16]

The decrease in the experimental value of the electron spin resonance *g* factor[2] was interpreted to indicate a significant transfer of spin from the oxygen to the amino group, as compared to that in unsubstituted phenoxyl radical. This spin delocalization has been further corroborated by resonance Raman studies of the vibrational frequencies[7−9] which imply that in water PAP is closer to the partial quinoid structure of *p*-benzosemiquinone radical anion than to the unsubstituted phenoxyl-like structure that is adopted by most other para-substituted phenoxyl radicals.

ENDOR-TRIPLE spectra have been used[4] to further determine the signs of the hfcc in PAP. That study[4] was undertaken to augment earlier ESR work[17] on the presumably closely related 2,6-di-*tert*-butyl derivative of PAP which reported a significant temperature dependence of the amino hydrogen couplings $a(H_N)$ but little temperature dependence of $a$(N) itself. Analysis of this data with the aid of semiempirical MO theory[18] led to the conclusion that the radical has a planar equilibrium structure, with the observed temperature dependence arising from considerable freedom for large amplitude torsional motions of the amino group that leads to a substantial vibrational averaging correction for $a(H_N)$. However, evidence against a large vibrational averaging correction to $a(H_N)$ comes from the hfcc observed[8] for PAP deuterated at the amino site which is found to have deuterium couplings that, after correcting for the known difference in nuclear gyromagnetic ratios, are close to those of the amino hydrogens in PAP itself.

Previous theoretical studies have failed to give a satisfactory description of PAP. A planar geometry with an essentially benzenoid ring and an amino group not significantly involved in the conjugation was found in a theoretical ROHF/[32|2] study.[14] However, a structure of that nature is inconsistent[10,19] with the experimentally observed vibrational frequencies, spin distribution, and chemical properties. A higher level theoretical UNO-CAS(7,7)/6-31G* study[15] has found the radical to be highly nonplanar, with a pyramidalization angle $\theta$ between the CN bond and the $NH_2$ plane of 42.7°. That work[15] finds PAP to be similar in structure to most other para-substituted phenoxyl radicals, in contradiction to the inferences obtained in several experimental studies.[2,7−10,19]

A good discussion has been given[3] on the importance of PAP as a key intermediate in the oxidation of *p*-aminophenol in biological systems. Also, a comprehensive summary has been provided[19] on the available spectroscopic and chemical information on PAP as compared to that on the phenoxyl radical, *p*-benzosemiquinone anion, and other closely related radicals. It has been further argued[19] that interactions with solvent are important in determining the observed properties of PAP in water.

The present work reports theoretical studies designed to further elucidate the structure and properties of PAP and to help resolve the unsettled issues noted above. In view of the conflicting conclusions obtained in previous studies, a prerequisite for achieving this goal will clearly be to first identify levels of theory that are capable of producing results consistent with the unambiguous experimental findings. We particularly

10.1021/jp992811z CCC: $18.00 
Published on Web 11/09/1999

**TABLE 1: Geometry[a] and Inversion Barrier[b] in *p*-Aminophenoxyl Radical as Obtained by Various Computational Methods**

| method | basis set | R($C_1O$) | R($C_1C_2$) | R($C_2C_3$) | R($C_3C_4$) | R($C_4N$) | $\theta^c$ | $\Delta E_{inv}{}^b$ |
|---|---|---|---|---|---|---|---|---|
| | | | | PAP Equilibrium | | | | |
| ROHF | 3-21G | 1.364 | 1.388 | 1.373 | 1.400 | 1.367 | 0 | 0 |
| UHF | 3-21G | 1.305 | 1.420 | 1.380 | 1.409 | 1.377 | 0 | 0 |
| UHF | 6-31G* | 1.251 | 1.439 | 1.382 | 1.412 | 1.395 | 42.8 | 1.55 |
| UHF | 6-311G(2d,p) | 1.243 | 1.437 | 1.375 | 1.408 | 1.394 | 44.3 | 1.74 |
| CAS(9,8) | 6-311G(2d,p) | 1.225 | 1.454 | 1.367 | 1.415 | 1.389 | 41.8 | 2.71 |
| BPW91 | 6-31G* | 1.263 | 1.462 | 1.379 | 1.428 | 1.378 | 26.4 | 0.16 |
| BPW91 | 6-311G(2d,p) | 1.257 | 1.458 | 1.373 | 1.423 | 1.375 | 27.9 | 0.18 |
| | | | | PAP Constrained Planar | | | | |
| UHF | 6-31G* | 1.250 | 1.439 | 1.380 | 1.413 | 1.374 | 0 | 0 |
| BPW91 | 6-31G* | 1.263 | 1.462 | 1.379 | 1.428 | 1.371 | 0 | 0 |
| | | | | PAP·4w Equilibrium | | | | |
| UHF | 6-31G* | 1.244 | 1.444 | 1.374 | 1.417 | 1.374 | 34.6 | 0.48 |
| BPW91 | 6-31G* | 1.284 | 1.453 | 1.377 | 1.433 | 1.357 | 0 | 0 |

[a] Bond distances given in Å and angles in degrees. [b] Energy barrier to inversion, i.e., energy difference between the actual optimum geometry and the constrained planar optimized geometry, given in kcal/mol. [c] Angle between the CN bond and the $NH_2$ plane.

focus in this work on obtaining the first satisfactory theoretical account of the observed fundamental vibrational frequencies and hfcc.

## Computational Methods

Restricted open-shell Hartree−Fock (ROHF), unrestricted Hartree−Fock (UHF), and spin-restricted multiconfiguration self-consistent-field complete active space (CAS) calculations were carried out with the GAMESS program.[20] Previous UHF calculations[15] have indicated that the seven $\pi$ natural orbitals on oxygen and the ring carbon atoms have occupations significantly different from zero or two, indicating that nondynamical electron correlations among them may be important. For completeness, we also included the approximately doubly occupied $\pi$ orbital on nitrogen to obtain an active space consisting of all nine $\pi$ electrons distributed among eight $\pi$ orbitals (or their descendants in the case of nonplanar geometries) in CAS(9,8) calculations.

Density functional calculations were carried out with the Gaussian-94 program[21]. The BPW91 method, which combines Becke's 1988 exchange functional[22] with the Perdew−Wang 91 correlation functional,[23] was used for structural characterization. This method has previously[24] been found to provide a good description of the vibrational frequencies in the isoelectronic *p*-benzosemiquinone radical anion.

Energetic, geometric, and force field evaluations were obtained with the ROHF, UHF, CAS, and BPW91 methods using the split-valence 3-21G set,[25] the split-valence plus heavy-atom polarization 6-31G* set,[26,27] and the extended 6-311G-(2d,p) set.[28,29] Vibrational frequencies were obtained either from analytical second derivatives (ROHF, UHF, and BPW91) or analytical first derivatives with slightly displaced nuclei (CAS), each evaluated at the respective computed local minimum geometry. The composition of each normal mode in terms of local mode contributions was obtained by the total energy distribution method.[30]

None of the above-mentioned methods or basis sets describe spin densities very well. However, there is evidence[31−34] that the B3LYP method, which combines Becke's exchange functional,[35] with the Lee−Yang−Parr correlation functional,[36] often performs well for spin densities. So for hfcc evaluation we used the B3LYP method as implemented in Gaussian-94[21] together with a [631|41] basis set[37] that has previously been specially designed for this property.

Hydrogen bond energies, obtained as the energies required to dissociate the weakly bound water molecules from the PAP moiety, were corrected for basis set superposition error by the widely-accepted full counterpoise method.[38,39]

## Results and Discussion

**Geometrical Structure.** Experimental evidence[2,4,7−10] on PAP in water or ethanol solution is all consistent with a planar $C_{2v}$ structure, but does not necessarily preclude the possibility of a lower symmetry $C_s$ structure corresponding to pyramidalization at the nitrogen center to bend the amino hydrogens out of plane. Because previous studies[14,15] have indicated that the finding of whether the radical is planar or nonplanar is sensitive to the level of computation, we first carried out a survey of the equilibrium geometries predicted by various methods. The results are summarized in Table 1.

With a small 3-21G basis set, both ROHF and UHF predict planar structures having benzenoid-like ring distances. They differ primarily in that ROHF finds a long CO bond distance characteristic of a single bond, while UHF gives a shorter distance indicating partial double-bond character that allows the oxygen to participate in the conjugated system.

With larger 6-31G* and 6-311G(2d,p) basis sets, UHF finds a considerable shortening of the CO bond, bringing it closer to a typical double-bond distance, some alternation of the ring carbon distances toward a partial quinoid structure, and some lengthening of the CN bond. The latter is apparently enough to essentially remove the CN bond from participation in the conjugation, thus allowing for pyramidalization by over 40° at the nitrogen center and leading to a significant barrier to inversion of more than 1.5 kcal/mol. However, it should be noted that UHF methods may be unreliable as a result of severe spin contamination because $\langle S^2 \rangle \sim 1.3$ with all basis sets considered, as compared to the value 0.75, characteristic of a pure doublet spin state.

Including nondynamical $\pi$-space correlation with the CAS-(9,8)/6-311G(2d,p) method gives a still shorter CO bond, a more quinoid-like ring structure, and a highly pyramidalized nitrogen center with a large 2.7 kcal/mol barrier to inversion.

BPW91 density functional calculations with 6-31G* and 6-311G(2d,p) basis sets, on the other hand, give a very different structural prediction. Most notably, the CO bond is somewhat longer than those with large basis UHF calculations and the CN bond is a little shorter, reducing the pyramidalization angle at nitrogen to about 27°. The inversion barrier is considerably reduced to less than 0.2 kcal/mol. Thus, as discussed in more detail below, the equilibrium structure corresponding to this computational model should actually be regarded as quasi-planar

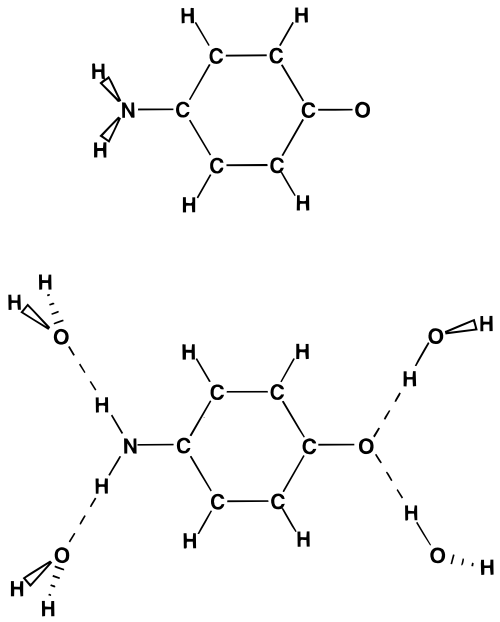

**Figure 1.** Structure of *p*-aminophenoxyl radical without and with hydrogen-bonded water molecules.

with large amplitude motion corresponding to $-NH_2$ pyramidalization in a low-barrier double-well potential.

The inversion barriers noted above were obtained by comparing total electronic energies of the actual calculated equilibrium structures with those of optimized structures obtained under the artificial constraint of planar $C_{2v}$ symmetry. The geometries for two of these constrained structures are reported in the middle section of Table 1. Both for UHF/6-31G*, which has a substantial inversion barrier, and for BPW91/6-31G*, which has a very small inversion barrier, the only significant change in the planar form is a shortening of the CN bond distance, by 0.021 Å in the former and 0.007 Å in the latter.

We now consider the possibility that perturbations due to solvent effects might alter the structural predictions. In this connection, we note that analogous calculations on the *p*-benzosemiquinone radical anion[24] have found that up to four water molecules can form strong hydrogen bonds, two at each oxygen atom. Accordingly, we consider here a cluster in which four water (w) molecules are coordinated to PAP. Two waters acting as hydrogen-bond donors are bound as HOH···O···HOH at the oxygen site with essentially linear hydrogen bonds lying in the plane, but having dangling terminal hydrogens with one above and one below the plane. The other two waters acting as hydrogen bond acceptors are bound as $H_2O$···HNH···$OH_2$ at the amino site, each water symmetrically having one hydrogen above and one below the local amino plane. The result, as shown in Figure 1, is a supermolecule cluster hereafter designated as PAP·4w.

With UHF/6-31G*, formation of the hydrogen bonds reduces the pyramidalization angle at nitrogen only slightly but leads to significant shortening of the CN bond length and reduction of the inversion barrier. The same general features are also found with BPW91/6-31G*, which produces an essentially planar PAP·4w structure of $C_2$ symmetry. Note that upon hydrogen bond formation UHF predicts a slight shortening of the CO bond while BPW91 instead predicts significant lengthening.

The slight deviation from strict $C_{2v}$ to the lower $C_2$ symmetry in the essentially planar PAP·4w supermolecule found by the BPW91/6-31G* calculation is due to the orientations of the terminal hydrogens on the two water molecules coordinated at the oxygen site. These dangle one above and one below the nominal plane, giving a structure slightly more stable than a strict $C_{2v}$ arrangement that would necessarily constrain these terminal hydrogens to lie in the molecular plane. However, previous studies on *p*-benzosemiquinone radical anion[24] have indicated that the relative orientations of such dangling hydrogens have very little influence on the properties of the central moiety of interest, and it is reasonable to assume that the same holds true here. The central PAP substructure moiety in PAP·4w with $C_2$ symmetry is very nearly planar, having all torsion angles within 0.3° of planarity. It is thus always possible to easily identify vibrational modes which derive from their strict planar $C_{2v}$ counterparts, and we henceforth discuss PAP·4w in terms of a quasi-$C_{2v}$ description.

For comparison, BPW91/6-31G* calculations were also carried out on intermediate PAP·2w supermolecules having two water molecules both bound at one end or the other. For the case of both waters bound at the oxygen site, the amino pyramidalization angle was reduced to 16.0°, as compared to the 26.4° found for the isolated molecule. For the case of both waters bound at the amino site, the optimum geometry was found to be strictly planar. Thus, all the hydrogen-bonded waters help to promote planarity, with the amino-bound waters being more effective at this than the oxygen-bound waters.

For the BPW91/6-31G* structure of PAP·4w the hydrogen bond strength is calculated to be an average of 5.4 kcal/mol per water molecule. This is a little stronger than that in water dimer where BPW91/6-31G* calculations on the usual single-donor single-acceptor structure give 4.5 kcal/mol, as compared to the semiexperimental result[40] of 5.4 kcal/mol for the electronic contribution. Comparison to analogous calculations on the intermediates having just two bound water molecules indicates that the individual hydrogen bond strengths in PAP·4w are independent and additive to better than 10% and that the waters at the oxygen site are each ~1 kcal/mol more strongly bound than each of those at the amino site.

Comparing Mulliken population analyses of the BPW91/6-31G* calculations on PAP and PAP·4w suggests that each oxygen-bound water withdraws 0.03 e and each amino-bound water donates 0.07 e to the central PAP moiety, leaving it with a net charge of 0.07 e and giving the complex an incipient partial zwitterionic character.

**Vibrational Frequencies.** Fundamental vibrational frequencies have been determined from the full harmonic force field of each calculation. Reasonable choices were tried for force constant scaling factors in the Hartree−Fock[41] and CAS[42] calculations. However, even with scaling none of these calculations were able to provide a satisfactory account of the experimentally determined results.[7−9] In particular, the CN stretch mode always remained below 1300 $cm^{-1}$ whereas experimentally it is found above 1400 $cm^{-1}$. We therefore do not present Hartree−Fock or CAS vibrational results in any detail.

The BPW91/6-31G* calculations, on the other hand, give good agreement with experimental vibrational results, even without any force field scaling. Table 2 shows the results for fundamental modes that are candidates for strong enhancement in resonance Raman spectroscopy, i.e., totally symmetric modes other than hydrogenic stretches.

Calculated BPW91/6-31G* results for PAP, constrained planar PAP, and PAP·4w each give a sufficiently good account of the observed totally symmetric fundamental vibrational frequencies to confirm all the assignments previously proposed in the experimental work.[7−9] The PAP·4w results are extremely

**TABLE 2: Frequencies (in cm$^{-1}$) for Totally Symmetric Fundamental Vibrational Modes in *p*-Aminophenoxyl Radical**

| | | fundamental frequency | | | | $-NH_2$ to $-ND_2$ shift | | | |
|---|---|---|---|---|---|---|---|---|---|
| label | mode[a] | PAP equilibrium nonplanar | PAP constrained planar | PAP·4w equilibrium planar | expt[b] | PAP equilibrium nonplanar | PAP constrained planar | PAP·4w equilibrium planar | expt[b] |
| 6a | CCC bend | 454 | 454 | 462 | 474 | −8 | −8 | −11 | |
| 1 | ring breathe | 766 | 767 | 778 | | −14 | −14 | −14 | |
| 18a | CC stretch | 810 | 811 | 827 | 824 | −5 | −6 | −7 | −6 |
| 12 | ring bend | 959 | 958 | 973 | | 0 | 0 | 0 | |
| 9a | CH bend | 1157 | 1158 | 1174 | 1168 | −6 | −8 | −11 | −8 |
| 19a | CH bend | 1320 | 1326 | 1339 | | 35 | 35 | 23 | |
| | CN stretch | 1437 | 1440 | 1441 | 1434 | 7 | 11 | 10 | 13 |
| 7a | CO stretch | 1527 | 1528 | 1526 | 1518 | 0 | 0 | 2 | −6 |
| 8a | CC stretch | 1611 | 1612 | 1634 | 1636 | 5 | 7 | 5 | 6 |
| | $\delta NH_2$ | 1647 | 1645 | 1669 | 1673 | −481 | −479 | −479 | −495 |

[a] Approximate description, giving most important local mode in each normal mode. [b] From resonance Raman measurements in $H_2O$, refs 8 and 9.

good in this connection, with a mean absolute error of only 6 cm$^{-1}$ from experiment in water, as compared to 15 cm$^{-1}$ for PAP and 16 cm$^{-1}$ for constrained planar PAP. This lends some support to the physical validity of an essentially planar structure in water. The three models considered in Table 2 all give about equally good accounts of the observed isotope shifts for amino hydrogen to deuterium substitution.

The BPW91/6-31G* normal mode dominated by $-NH_2$ inversion is calculated at 383 cm$^{-1}$ in PAP and at 284i cm$^{-1}$ in constrained planar PAP. There are no other imaginary frequencies in constrained planar PAP, verifying that it is indeed the transition state for this inversion. Recall that the corresponding barrier to inversion of the $-NH_2$ group in PAP is 0.16 kcal/mol, as calculated from the electronic energy difference. This barrier still remains small at 0.24 kcal/mol when the difference in zero-point vibrational energy between the equilibrium nonplanar and constrained planar structures is also included (omitting the $-NH_2$ inversion normal mode from both forms). The calculated harmonic frequency of 383 cm$^{-1}$ for the inversion mode in equilibrium nonplanar PAP corresponds to a zero-point energy $^1/_2h\nu$ of 0.55 kcal/mol that is larger than the calculated inversion barrier. Thus, as noted earlier, the equilibrium structure in this case should actually be regarded as quasi-planar and the calculated harmonic frequency has little physical relevance.

The situation is more complicated in PAP·4w, where the $-NH_2$ inversion local mode does not dominate any particular normal mode. It is instead found to be distributed among several normal modes, mostly in those calculated at 28, 53, and 263 cm$^{-1}$. However, these normal modes are primarily solvent in character and are not very meaningfully characterized here because they would undoubtedly be considerably altered if further shells of bulk solvent molecules were included in the calculation. Thus, we only make the qualitative conclusion that formation of hydrogen bonds leads to loss of the identity of the $-NH_2$ inversion local mode through mixing into low-frequency normal modes having considerable solvent character.

With BPW91/6-31G* the normal mode dominated by $-NH_2$ torsion is calculated at 407 cm$^{-1}$ in nonplanar equilibrium PAP and at 424 cm$^{-1}$ in constrained planar PAP. However, just as for the inversion mode, in planar equilibrium PAP·4w the $-NH_2$ torsion local mode does not dominate any particular normal mode. Instead, it is distributed mostly among five different normal modes. Slightly over half of its contributions are found in normal modes at 27, 73, and 280 cm$^{-1}$ that are primarily solvent in character and would undoubtedly be considerably altered if more bulk solvent molecules were included in the calculation. Slightly under half of its contributions are found in normal modes at 757 and 834 cm$^{-1}$ that are primarily CH wag in character and which are probably characterized reasonably well. Thus, we make the qualitative conclusion that formation of hydrogen bonds also leads to loss of the identity of the $-NH_2$ torsion local mode, here due partly to mixing with low-frequency solvent modes and partly to mixing with higher frequency CH wag modes.

**TABLE 3: B3LYP/[631|41] Isotropic Hyperfine Coupling Constants (in G) Calculated for Several Optimized BPW91/6-31G* Structures of *p*-Aminophenoxyl Radical**

| nucleus | PAP equilibrium nonplanar | PAP constrained planar | PAP·4w equilibrium planar | expt[a] |
|---|---|---|---|---|
| $a(^{13}C_1)$ | −10.0 | −9.8 | −4.7 | |
| $a(^{13}C_2)$ | 5.5 | 5.3 | 2.2 | |
| $a(^{13}C_3)$ | −6.6 | −6.2 | −3.2 | |
| $a(^{13}C_4)$ | 7.6 | 6.9 | 2.9 | |
| $a(^{17}O)$ | −8.3 | −8.3 | −7.9 | |
| $a$(N) | 3.7 | 2.0 | 3.1 | 5.2 |
| $a(H_2)$ | −5.3 | −5.2 | −3.6 | −2.7 |
| $a(H_3)$ | 1.1 | 0.9 | −0.5 | −1.8 |
| $a(H_N)$ | −1.5 | −4.3 | −5.7 | −5.6 |

[a] Values from ESR measurements in $H_2O$, ref 8. Signs taken from ENDOR/TRIPLE measurements in EtOH, ref 4.

**Isotropic Hyperfine Coupling Constants.** The B3LYP/[631|41] hfcc calculated for optimized BPW91/6-31G* structures are reported in Table 3. Ring atoms are numbered starting at 1 for the carbon bonded to oxygen, moving up to 4 for the carbon bonded to nitrogen. Thus, $C_6$ is equivalent to $C_2$ and $C_5$ is equivalent to $C_3$.

No experimental data are available for the carbon or oxygen atom couplings. The calculations predict that hydrogen bond formation leads to large changes in all the $^{13}C$ couplings but only a small change in the $^{17}O$ coupling. Hydrogen bond formation also significantly affects the calculated ring hydrogen couplings. The $a(H_2)$ value becomes less negative and $a(H_3)$ becomes more negative, leading to considerable improvement of both calculated couplings as compared with the experimental results in water.

The amino group couplings are particularly interesting. For nitrogen the calculations indicate a decrease in the coupling due to the geometry change from nonplanar to planar, which is counterbalanced by an increase due to the formation of hydrogen bonds in the planar structure. Even in PAP·4w there remains a significant discrepancy of ~2 G between the calculated nitrogen coupling and the experimental results in water. For the amino hydrogen couplings, the calculations show a large shift upon

changing the geometry from nonplanar to planar and a smaller shift in the same direction due to the formation of hydrogen bonds to water molecules. The calculated amino hydrogen coupling for PAP·4w is in excellent but perhaps fortuitous agreement with the experimental result in water.

We now consider the possibility of vibrational-averaging corrections to the hfcc. It has already been seen that large amplitude motion can be expected for pyramidalization of the amino group. In the pyramidalized form, the SOMO will have some s character, giving significant positive direct contributions to all the hfcc. But in the planar geometry, this is a $\pi$-radical having no direct contribution from the SOMO to the Fermi contact spin density at any of the nuclei lying in the plane, so the planar couplings arise only from higher order contributions due to spin polarization and electron correlation. Therefore, vibrational averaging over the pyramidalization motion may provide significant corrections to the hfcc, especially for the amino group atoms. Before carrying out quantitative calculations, it is possible to make qualitative arguments on the signs of the corrections.

For isolated PAP having a nonplanar equilibrium structure, vibrational averaging over the amino pyramidalization motion will likely provide a correction in the direction corresponding to the constrained planar structure. Thus, the nitrogen coupling should become less positive and the amino hydrogen coupling should become more negative for PAP. For the planar PAP·4w structure, on the other hand, this motion should make the nitrogen coupling more positive and the amino hydrogen coupling less negative.

Torsion of the amino group is another possibility for large amplitude motion. For the nonplanar equilibrium PAP structure, amino torsion could lead to significant corrections for nitrogen and for amino hydrogen atoms. For the planar equilibrium PAP·4w structure, amino torsion would leave the nitrogen atom in the plane while rotating the amino hydrogens out of the plane, and therefore[18] a significant correction would be unlikely for nitrogen but could occur for hydrogen.

We have estimated hfcc corrections due to vibrational averaging by treating the $-NH_2$ pyramidalization and torsional motions separately as independent large-amplitude one-dimensional oscillators. A series of single-point calculations was carried out, changing either the pyramidalization or torsion angle by increments from its equilibrium value. The potential energy curves were characterized by spline fits to the respective series of calculated BPW91/6-31G* energies, and the hfcc by spline fits to the calculated B3LYP/[631|41] values. In most cases, it was assumed that all other structural parameters remained frozen at their equilibrium values during each of these large amplitude motions. However, in the case of pyramidalization for isolated PAP, which has a nonplanar equilibrium structure, a more detailed study was made by carrying out constrained optimizations of all other geometrical parameters for each fixed value of $\theta$.

The average hfcc in each of a number of low-lying vibrational levels was determined by numerical solution[43] of the corresponding one-dimensional vibrational Schrödinger equation. Because only estimates of the vibrational corrections were being sought, the reduced mass for each motion was simply taken to be a constant, as determined from the reciprocal of the corresponding Wilson G-matrix element evaluated at the reference equilibrium geometry. Final averaging of the hfcc over the available vibrational levels at a given temperature was carried out assuming a Boltzmann distribution of populations.

**TABLE 4: Vibrational Corrections at 300 K to B3LYP/[631|41] Isotropic Hyperfine Coupling Constants (in G) Calculated for Amino Group Atoms in Optimized BPW91/6-31G* Structures of *p*-Aminophenoxyl Radical (Temperature Derivatives of the hfcc (in mG/K) and Hydrogen−Deuterium Isotope Shifts (in G) Are Also Given at 300 K)**

| nucleus | contribution | PAP | PAP·4w | expt |
|---|---|---|---|---|
| $a$(N) | equilibrium | 3.7 | 3.1 | |
| | Δ pyram | −0.3 | 0.5 | |
| | Δ torsion | −0.1 | 0.0 | |
| | estimated total | 3.3 | 3.5 | 5.2[a] |
| $a(H_N)$ | equilibrium | −1.5 | −5.7 | |
| | Δ pyram | −0.3 | 0.7 | |
| | Δ torsion | 0.1 | 0.1 | |
| | estimated total | −1.8 | −4.9 | −5.6[a] |
| d$a$(N)/d$T$ | pyram | 1.2 | 0.2 | |
| | torsion | −0.1 | 0.0 | |
| | estimated total | 1.1 | 0.2 | ∼0[b] |
| d$a(H_N)$/d$T$ | pyram | 2.2 | 0.4 | |
| | torsion | 0.1 | 0.1 | |
| | estimated total | 2.3 | 0.5 | ∼10[b] |
| $a(H_N)-a(D_N)$ | pyram | −0.04 | 0.11 | |
| | torsion | 0.02 | 0.03 | |
| | estimated total | −0.02 | 0.14 | 0.19 ± 0.07[c] |

[a] Values from ESR measurements in $H_2O$, ref 8. Signs taken from ENDOR/TRIPLE measurements in EtOH, ref 4. [b] Obtained for 2,6-di-*tert*-butyl derivative of PAP in ref 17. See text for discussion. [c] Values from ESR measurements in $H_2O$, ref 8.

Total hfcc values corresponding to averaging over both pyramidalization and torsion motions were estimated by assuming the separate corrections for each of these motions to be independent and additive. Significant vibrational corrections to hfcc were found only for the amino group atoms. Results for the equilibrium geometry, for the vibrational corrections (Δ) at $T = 300$ K, and for the estimated total couplings at $T = 300$ K are reported in the top sections of Table 4.

For the nitrogen coupling the vibrational corrections are modest, amounting to −0.4 G for PAP and 0.4 G for PAP·4w. The total result for PAP·4w is now in a little better agreement with the experimental value in water. For the amino hydrogen coupling, there is little net correction for PAP but a more substantial 0.8 G for PAP·4w, which leads to slightly worse but still reasonable agreement with experiment.

Our main motivation for carrying out vibrational averaging corrections was to investigate an early experimental finding[17] of significant temperature dependence of the amino hydrogen hfcc. While experimental data were actually given only for the 2,6-di-*tert*-butyl derivative of PAP, it has been clearly implied[4,17,18] that similar behavior was to be expected for the presumably closely related *p*-aminophenoxyl radical itself. It was reported[17] that the slope d$a$/d$T$ of the amino hydrogen coupling is essentially constant over a wide range of temperatures both below and above 300 K, and amounts to 11.85 mG/K in *n*-hexane, 9.84 mG/K in ether, and 10.27 mG/K in ethanol. The close similarity of these results in different solvents suggests that the observed temperature dependence is generic and not related to any hydrogen bonding or other specific solute−solvent interactions.

It is also remarkable that no significant accompanying temperature dependence was found[17] for $a$(N). From the published graph, we can estimate a value of d$a$(N)/d$T \lesssim 0.1$ mG/K, which is 2 orders of magnitude smaller than the reported values for d$a(H_N)$/d$T$. This lack of nitrogen temperature dependence was used[18] to argue that the amino hydrogen

temperature dependence cannot arise from pyramidalization motions, but rather is probably due to torsional motions away from a planar equilibrium structure.

Our results on the hfcc temperature dependence are given in the middle sections of Table IV. It is interesting to note that the calculations indicate larger contributions from pyramidalization than from torsion to both $da(N)/dT$ and $da(H_N)/dT$. More importantly, it is clear that the calculated findings are unable to rationalize the reported observations.[17] For one thing, we obtain values for $da(H_N)/dT$ in both PAP and PAP·4w that are much smaller than the experimental report. For another thing, our calculated value for PAP is significantly different from that for PAP·4w which implies an important role for hydrogen-bonding effects on the result. Finally, we obtain values for $da(N)/dT$ that, while smaller, are still of the same order of magnitude as the corresponding values for $da(H_N)/dT$. Each of these findings is in qualitative disagreement with the experimental report.[17]

This complete lack of agreement with experiment on the temperature dependence of amino group couplings raises the question of whether or not our calculated vibrational averaging results are realistic. So as an independent test, we have considered the hydrogen−deuterium isotope shift for the amino hydrogen coupling. An ESR investigation[8] in water found, after correction of $a(D_N)$ for the known difference in deuterium and hydrogen nuclear gyromagnetic ratios to isolate just the mass effect, a small but significant experimental shift of 0.19 G for $a(H_N)-a(D_N)$, with a worst case maximum error of ±0.07 G. As shown in the bottom section of Table 4, we find that both pyramidalization and torsion make significant contributions to this isotope shift, leading to an estimated total shift of 0.14 G in PAP·4w that is in satisfactory agreement with the experimental value in water. This provides strong evidence that our treatment of vibrational-averaging corrections to the amino group hfcc is at least qualitatively correct.

## Conclusions

Computations based on Hartree−Fock and full $\pi$-space CAS methods give unsatisfactory accounts of the experimental vibrational frequencies of *p*-aminophenoxyl radical in water. This failure arises primarily from improper description of the CN bond by not allowing it to effectively participate in the conjugation. Computations based on the BPW91/6-31G* density functional method, on the other hand, give vibrational results for PAP that are in reasonable agreement with experiment. Inclusion of solvation effects through incorporation of hydrogen-bonded water molecules in a PAP·4w cluster further improves the agreement with experiment. The hydrogen-bonded water molecules promote planarity and strengthen the CN bond in this radical.

The B3LYP/[631|41] hydrogen atom hfcc are also in substantially better agreement with the experimental results in water when explicit hydrogen-bonded water molecules are included in the calculations, although the coupling at nitrogen is still somewhat underestimated. Vibrational averaging over pyramidalization and torsional motions of the amino group give small but not negligible corrections to the nitrogen and amino hydrogen couplings. The calculated vibrational corrections give no support to a significant temperature dependence for the amino hydrogen coupling. If the early experimental report of finding this temperature dependence in the 2,6-di-*tert*-butyl derivative of PAP is correct, then this suggests a breakdown in the implied assumption of similar behavior in unsubstituted PAP. We consequently recommend that this matter be experimentally examined in PAP itself. The calculated vibrational corrections do provide an excellent account of the small experimentally observed hydrogen−deuterium isotope shift of the amino hydrogen coupling.

**Acknowledgment.** Valuable discussions with Drs. G. N. R. Tripathi and R. H. Schuler are gratefully acknowledged. The research described herein was supported by the Office of Basic Energy Sciences of the Department of Energy. This is Contribution No. NDRL-4145 from the Notre Dame Radiation Laboratory.

## References and Notes

(1) Stegmann, H. B.; Schleffler, K. *Z. Naturforsch.* **1964**, *19b*, 537.
(2) Neta, P.; Fessenden, R. W. *J. Phys. Chem.* **1974**, *78*, 523.
(3) Josephy, P. D.; Eling, T. E.; Mason, R. P. *Mol. Pharm.* **1983**, *23*, 461.
(4) Scheffler, K.; Stegmann, H. B.; Ulrich, C.; Schuler, P. *Z. Naturforsch.* **1984**, *39a*, 789.
(5) Dixon, W. T.; Murphy, D. *J. Chem. Soc., Faraday Trans. 2* **1976**, *72*, 1221.
(6) Steenken, S.; Neta, P. *J. Phys. Chem.* **1981**, *86*, 3661.
(7) Tripathi, G. N. R.; Schuler, R. H. *J. Chem. Phys.* **1982**, *76*, 4289.
(8) Tripathi, G. N. R.; Schuler, R. H. *J. Phys. Chem.* **1984**, *88*, 1706.
(9) Sun, Q.; Tripathi, G. N. R.; Schuler, R. H. *J. Phys. Chem.* **1990**, *94*, 6273.
(10) Tripathi, G. N. R.; Schuler, R. H. *J. Chem. Soc., Faraday Trans.* **1993**, *89*, 4177.
(11) Lind, J.; Shen, X.; Eriksen, T. E.; Merényi *J. Am. Chem. Soc.* **1990**, *112*, 479.
(12) Bordwell, F. G.; Cheng, J.-P. *J. Am. Chem. Soc.* **1991**, *113*, 1736.
(13) Tanaka, K.; Sakai, S.; Tomiyama, S.; Nishiyama, T.; Yamada, F. *Bull. Chem. Soc. Jpn.* **1991**, *64*, 2677.
(14) Raymond, K. S.; Wheeler, R. A. *J. Chem. Soc., Faraday Trans.* **1993**, *89*, 665.
(15) Liu, R.; Zhou, X. *J. Phys. Chem.* **1993**, *97*, 9613.
(16) Wu, Y.-D.; Lai, D. K. W. *J. Org. Chem.* **1996**, *61*, 7904.
(17) Scheffler, K.; Stegmann, H. B. *Tetrahedron Lett.* **1964**, *40*, 3035.
(18) Stone, A. J.; Carrington, A. *Trans. Faraday Soc.* **1965**, *61*, 2593.
(19) Tripathi, G. N. R. *J. Phys. Chem.* **1998**, *102*, 2388.
(20) Schmidt, M. W.; Baldridge, K. K.; Boatz, J. A.; Elbert, S. T.; Gordon, M. S.; Jensen, J. H.; Koseki, S.; Matsunaga, N.; Nguyen, K. A.; Su, S. J.; Windus, T. L.; Dupuis, M.; Montgomery, J. A. *J. Comput. Chem.* **1993**, *14*, 1347.
(21) Frisch, M. J.; Trucks, G. W.; Schlegel, H. B.; Gill, P. M. W.; Johnson, B. G.; Robb, M. A.; Cheeseman, J. R.; Keith, T.; Petersson, G. A.; Montgomery, J. A.; Raghavachari, K.; Al-Laham, M. A.; Zakrzewski, V. G.; Ortiz, J. V.; Foresman, J. B.; Cioslowski, J.; Stefanov, B. B.; Nanayakkara, A.; Challacombe, M.; Peng, C. Y.; Ayala, P. Y.; Chen, W.; Wong, M. W.; Andres, J. L.; Replogle, E. S.; Gomperts, R.; Martin, R. L.; Fox, D. J.; Binkley, J. S.; Defrees, D. J.; Baker, J.; Stewart, J. P.; Head-Gordon, M.; Gonzalez, C.; Pople, J. A. *Gaussian 94*, Revision D.2; Gaussian, Inc.: Pittsburgh, PA, 1995.
(22) Becke, A. D. *Phys. Rev. A* **1988**, *38*, 3098.
(23) Perdew, J. P.; Wang, Y. *Phys. Rev. B* **1992**, *45*, 13244.
(24) Zhan, C.-G.; Chipman, D. M. *J. Phys. Chem.* **1998**, *102*, 1230.
(25) Binkley, J. S.; Pople, J. A.; Hehre, W. J. *J. Am. Chem. Soc.* **1980**, *101*, 939.
(26) Hehre, W. J.; Ditchfield, R.; Pople, J. A. *J. Chem. Phys.* **1972**, *56*, 2257.
(27) Hariharan, P. C.; Pople, J. A. *Theoret. Chim. Acta* **1973**, *28*, 213.
(28) Krishnan, R.; Binkley, J. S.; Seeger, R.; Pople, J. A. *J. Chem. Phys.* **1980**, *72*, 650.
(29) Frisch, M. J.; Pople, J. A.; Binkley, J. S. *J. Chem. Phys.* **1984**, *80*, 3265. Our calculations used six-component d functions rather than the five components originally specified for this set.
(30) Pulay, P.; Torok, F. *Acta Chim. Acad. Sci. Hung.* **1965**, *47*, 273.
(31) Barone, V. In *Recent Advances in Density Functional Methods*; Chong, D. P., Ed.; World Scientific Publishing: Singapore, 1995.
(32) Wetmore, S. D.; Boyd, R. J.; Eriksson, L. A. *J. Chem. Phys.* **1997**, *106*, 7738.
(33) Grafton, A. K.; Wheeler, R. A. *J. Phys. Chem. A* **1997**, *101*, 7154.
(34) O'Malley, P. J. *J. Phys. Chem.* **1998**, *102*, 248.
(35) Becke, A. D. *J. Chem. Phys.* **1993**, *98*, 5648.
(36) Lee, C.; Yang, W.; Parr, R. G. *Phys. Rev. B* **1988**, *37*, 785.
(37) Chipman, D. M. *J. Chem. Phys.* **1989**, *91*, 5455. In that work the [631|41] basis was labeled as [5s2p1d|3$^+$s1p] +diffuse sps.
(38) Boys, S. F.; Bernardi, F. *Mol. Phys.* **1970**, *19*, 553.

(39) van Duijneveldt, F. B.; van Duijneveldt-van de Rijdt, J. G. C. M.; Lenthe, J. H. *Chem. Rev*. **1994**, *94*, 1873.
(40) Curtiss, L. A.; Frurip, D. J.; Blander, M. *J. Chem. Phys.* **1979**, *71*, 2703.
(41) Pople, J. A.; Schlegel, H. B.; Krishnan, R.; DeFrees, D. J.; Binkley, J. S.; Frisch, M. J.; Whiteside, R. A.; Hout, R. F.; Hehre, W. J. *Int. J. Quantum Chem.* **1981**, *S15*, 269.
(42) Chipman, D. M.; Liu, R.; Zhou, X.; Pulay, P. *J. Chem. Phys.* **1994**, *100*, 5023.
(43) Truhlar, D. G. *J. Comput. Phys.* **1972**, *10*, 173.